Cardiovascular Pathology 40 (2019) 24–31

Contents lists available at ScienceDirect

Cardiovascular Pathology

Original Article

# Coronary high-signal-intensity plaques on $T_1$-weighted magnetic resonance imaging reflect intraplaque hemorrhage

Yasuyoshi Kuroiwa [a,b], Akiko Uchida [b], Atsushi Yamashita [b,*], Tosiaki Miyati [c], Kazunari Maekawa [b], Toshihiro Gi [b], Teruo Noguchi [d], Satoshi Yasuda [d], Takuroh Imamura [e], Yujiro Asada [b]

[a] Department of Radiological Technology, Koga General Hospital, 1749-4 Sudaki, Ikeuchi, Miyazaki 880-0041, Japan
[b] Department of Pathology, Faculty of Medicine, University of Miyazaki, 5200 Kihara, Kiyotake, Miyazaki 889-1692, Japan
[c] Faculty of Health Sciences, Institute of Medical, Pharmaceutical and Health Sciences, Kanazawa University, 5-11-80 Kodatsuno, Kanazawa 920-0942, Japan
[d] Department of Cardiovascular Medicine, National Cerebral and Cardiovascular Center, 5-7-1 Fujishiro-dai, Suita, Osaka 565-8565, Japan
[e] Department of Internal Medicine, Koga General Hospital, 1749-4 Sudaki, Ikeuchi, Miyazaki 880-0041, Japan

ARTICLE INFO

*Article history:*
Received 29 October 2018
Received in revised form 3 December 2018
Accepted 7 January 2019

*Keywords:*
Coronary artery
Erythrocyte
Intraplaque hemorrhage
Magnetic resonance imaging
$T_1$-weighted image

ABSTRACT

Coronary high-signal-intensity plaques (HIPs) detected by $T_1$-weighted magnetic resonance imaging are associated with future cardiovascular events. This study aimed to identify pathological findings reflecting HIPs in coronary arteries obtained from autopsy cases. Formalin-fixed hearts were imaged with noncontrast $T_1$-weighted imaging with a 1.5-T magnetic resonance system. We defined HIPs or non-HIPs as a coronary plaque to myocardial signal intensity ratio (PMR) of ≥1.4 or <1.4, respectively. We found HIPs in 4 of 37 (10.8%) hearts and analyzed 7 hearts in detail. The corresponding sections to HIPs ($n$=11) or non-HIPs ($n$=25) were histologically and immunohistochemically analyzed. We calculated the $T_1$ relaxation time of human venous blood *in vitro*. Plaque and necrotic core areas, and the frequency of intraplaque hemorrhage in HIPs were significantly larger/higher than those in non-HIPs. HIPs were immunopositive for CD68 (11/11), glycophorin A (10/11), and fibrin (11/11). Glycophorin-A-, matrix metalloprotease 9 (MMP9)-, and tissue factor-immunopositive areas were larger in HIPs than in non-HIPs. The PMR was positively correlated with glycophorin-A-, fibrin-, MMP9-, and tissue factor-immunopositive areas. Blood coagulation shortened the $T_1$ relaxation time of the blood and plasma, and the $T_1$ relaxation times in coagulated whole blood and erythrocyte-rich blood were significantly shorter than those in plasma. Coronary HIPs may reflect intraplaque hemorrhage and may be a novel marker for plaque instability and thrombogenic potential.



## 1. Introduction

Cardiovascular disease is a leading cause of death worldwide, and ischemic heart disease and stroke accounted for a combined 18 million deaths in 2015 [1]. There were an estimated 7 million acute myocardial infarctions and 100 million prevalent cases of ischemic heart disease in 2015. Although the age-standardized death rate from cardiovascular disease dropped globally from 1990 to 2010, progress has slowed over the last 5 years [1]. Most acute myocardial infarctions are triggered by a sudden morphological change in atherosclerotic plaques and subsequent thrombus formation. Therefore, development of noninvasive modalities that can predict future coronary events is important.

Coronary atherosclerosis can be assessed with computed tomography (CT), magnetic resonance imaging (MRI), or $^{18}$F-fluorodeoxyglucose positron emission tomography. In a previous study, acute coronary syndrome developed in 20% of patients with positive remodeled and low-attenuation coronary plaques on CT angiography within 30 months [2]. $^{18}$F-fluorodeoxyglucose positron emission tomography can quantify atherosclerotic inflammation, and the target to background ratio measured in the ascending aorta is associated with subsequent cardiovascular events independent of the Framingham risk score [3,4]. Coronary high-signal-intensity plaques (HIPs) on non-contrast $T_1$-weighted imaging ($T_1$WI) is considered a predictor of coronary events. We previously identified a plaque to myocardial signal intensity ratio (PMR) of 1.4 as the optical cutoff for predicting prognosis in patients with suspected or known coronary artery disease [5]. We also showed that, during the follow-up period (median: 55 months), one fourth of patients with a PMR ≥1.4 developed coronary events. HIPs are associated with intravascular ultrasound-derived low attenuation and positive remodeling, low CT density [6], and the presence of lipid-rich plaques, macrophage accumulation, cholesterol crystals, and healed plaque rupture as assessed by optical coherence tomography (OCT) [7]. However, the underlying pathological and biological

*Abbreviations:* bandwidth, BW; echo time, TE; flip angle, FA; millisecond, ms; number of excitations, NEX; repetition time, TR.

* Corresponding author.
*E-mail address:* atsushi_yamashita@med.miyazaki-u.ac.jp (A. Yamashita).

https://doi.org/10.1016/j.carpath.2019.01.002
1054-8807/

characteristics in coronary HIPs remain unclear owing to a lack of histopathological analysis.

Therefore, this study aimed to identify which coronary HIPs on $T_1$WI are reflected by plaque pathology.

## 2. Methods

### 2.1. In vitro MRI of the human heart

We performed *in vitro* MRI of hearts that were obtained from 37 autopsy cases, which were performed within 5 h after death. We found HIPs, as defined below (2.4. Image and data analysis) in 4 of 37 (10.8%) hearts. We also analyzed 7 hearts (5 men and 2 women; 66–80 years) in detail. The cause of death in the autopsy cases included the following: acute myocardial infarction (AMI) ($n$=2), interstitial pneumonia ($n$=2), viral pneumonia ($n$=1), lung cancer ($n$=1), and sepsis ($n$=1). Supplementary Table 1 shows the clinical characteristics of patients with AMI and non-AMI patients. The hearts from the 7 autopsy cases were perfused with 20% buffered formalin to remove intracoronary clots. The formalin-fixed hearts were rinsed with water and then submerged in water in a plastic container. *In vitro* MRI was performed 2 to 5 days after fixation and involved a 1.5-T superconducting system combined with an 8-channel knee-phased array coil (Signa Excite HDxt; General Electric Medical Systems, Waukesha, WI, USA) equipped with 33 mT/m, 120 mT/m/ms gradients. We acquired three-dimensional fast spoiled gradient-recalled acquisition in the steady-state sequence $T_1$WI with fat suppression using the following parameters: repetition time (TR), echo time (TE), and flip angle of 14.8 ms, 2.0 ms, and 15°, respectively; number of excitations (NEX), two; and receiver bandwidth (BW), ±62.5 kHz. Three-dimensional fast-spin echo-cube sequence $T_2$-weighted imaging ($T_2$WI) with fat suppression was acquired at a TR and TE of 2.000 ms and 90 ms, respectively. Other parameters included the following: NEX, six; echo train length, 80; and receiver BW, ± 31.2 kHz. Further MRI parameters included a field of view of 140×140 mm, matrix of 320×320, and slice thickness of 1.2 mm. All images were acquired at room temperature (22°C). The Ethics Committee of Miyazaki University approved the study protocol (approval no. 2013-139).

### 2.2. Immunohistochemistry of the human coronary artery

Coronary arteries were cut at 4-mm intervals and embedded in paraffin. Investigators (Y.K., A.U., A.Y., and K.M.) selected magnetic resonance images with curved multiplanar reconstruction and corresponding hematoxylin–eosin-stained histological sections based on the length from the orifice, the shape of the plaque, and the presence of branches. We selected a total of 36 images, including the right coronary artery ($n$=13), left main coronary trunk ($n$=4), left anterior descending artery ($n$=11), and left circumflex artery ($n$=8). The corresponding sections (3 μm) to MRI were stained with Berlin blue (hemosiderin) and with antibodies against α-smooth muscle actin (SMA) (DAKO, Glostrup, Denmark), CD68 (DAKO), CD163 (macrophage haptoglobin–hemoglobin complex receptor; Leica Microsystems, Newcastle upon Tyne, UK), fibrin (Accurate Chemical & Scientific Corp., Westbury, NY, USA), glycophorin A (an erythrocyte protein; DAKO), matrix metalloproteinase 9 (MMP9) (Daiichi Fine Chemical Co., Ltd., Takaoka, Japan), and tissue factor (an initiator of blood coagulation; Abcam Plc., Cambridge, UK). The sections were then stained with Envision, anti-mouse immunoglobulin G, or anti-rabbit secondary antibody and horseradish peroxidase connected with a polymer (DAKO). Horseradish peroxidase activity was visualized using 3,3′-diaminobenzidine tetrahydrochloride and the sections were faintly counterstained with Meyer's hematoxylin. Immunostaining controls included nonimmune mouse or rabbit immunoglobulin G instead of the primary antibodies. The size of plaques and area of the necrotic core were measured in sections under a microscope using NIS-Element-D 3.2 image analysis software (Nikon, Tokyo, Japan). Intraplaque hemorrhage was defined as the focus of extravasation of intact erythrocytes in plaques with a hematoxylin–eosin stain and immunopositivity for glycophorin A [8]. Immunopositive areas of α-SMA, CD68, CD163, fibrin, glycophorin A, MMP9, and tissue factor or Berlin-blue-dye-positive areas were semiquantified using Win Roof color image analysis software 10 (Mitani, Fukui, Japan). These factors are expressed as ratios of positively stained area per plaque area.

### 2.3. In vitro blood MRI

To examine the contribution of blood contents or blood coagulation to HIPs on $T_1$WI, we performed in vitro blood MRI. The Ethics Committee of Miyazaki University approved the in vitro study protocol (approval no. 2015-147). Blood samples from healthy volunteers were collected from the median cubital vein into 3.8% sodium citrate (9:1, v/v) after informed consent. After centrifugation at 1800×$g$ for 10 min, plasma and plasma-removed centrifuged blood were separated. The number of blood cells was measured with a blood cell counter (XE-1800i; Sysmex, Kobe, Japan). Aliquots of 1200 μl of whole blood, plasma, and plasma-removed centrifuged blood were transferred to Eppendorf tubes, and blood clotting was induced by 150 μl of human placental tissue factor (Thromborel S; Sysmex) and 150 μl of $CaCl_2$ (100 mM). Two minutes after pipetting, the coagulated blood and noncoagulated blood (1500 μl) were imaged with a 1.5-T superconducting system combined with an 8-channel HD knee-phased array coil (Signa Excite HDxt; General Electric Medical Systems, Waukesha, WI, USA). The Eppendorf tubes with blood samples were placed in a 7.5% agarose gel phantom in the 1.5-T superconducting system using an 8-channel knee-phased array coil (Signa Excite HDxt; General Electric Medical Systems, Waukesha, WI, USA). The localizer consisted of fast, multislice, and multistack (axial, sagittal, and coronal images) segmented fast gradient-echo localizer scans of the blood samples (TR, 5.5 ms; TE, 1.6 ms; flip angle, 30°; field of view, 260×260 mm; BW, ± 31.25 kHz; matrix, 256×256; slice thickness, 3.0 mm). From axial images of the blood samples, a second sagittal and coronal scout with a reduced slice thickness (1 mm) was obtained along its major axis. Spin echo sequence $T_1$WIs were acquired at TE 13 ms, TR 400 ms, and NEX 2 and at TE 13 ms, TR 800 ms, and NEX 1. Other parameters included a BW of ±15.63 kHz and a matrix of 256×256. All images were acquired at 22°C.

### 2.4. Image and data analysis

MRI scans of coronary arteries were analyzed using OsiriX v.3.9.4 32-bit [9]. A curved muliplanar reconstruction algorithm was used to virtually uncoil the coronary artery wall from the volume data obtained from high-resolution three-dimensional $T_2$WI and $T_1$WI. Cursors for regions of interest were placed within coronary arterial walls with plaques to measure cross-sectional areas and signal intensities (Image J, U.S. National Institutes of Health, Bethesda, MD, USA). The signal intensity of the PMR was defined as the signal intensity of the coronary plaque divided by the signal intensity of adjacent cardiac muscle on $T_1$WI. Plaques with a maximum PMR ≥1.4 were defined as HIP ($n$=11), whereas plaques with a maximum PMR <1.4 were defined as non-HIP ($n$=25). We excluded thrombotic plaques in this study because a thrombus shows a high signal intensity on $T_1$WI. $T_1$ values of blood and plasma were calculated using the MRI Analysis calculator plug-in for Image J.

### 2.5. Statistical analysis

All data are presented as mean ± standard deviation or as individual dots. Differences for individual groups were tested using the Mann–Whitney $U$ test or one-way analysis of variance with a multiple

comparison test (GraphPad Prizm 6; GraphPad Software Inc., San Diego, CA, USA). Fisher's Exact Test was used for contingency table analysis. A value of $P<.05$ was considered statistically significant.

## 3. Results

We compared the histological findings of 11 HIPs (PMR ≥1.4) and 25 non-HIPs (PMR <1.4) with hematoxylin–eosin staining. Plaque and necrotic core areas in HIPs were significantly larger than those in non-HIPs (Fig. 1A and B). The frequency of intraplaque hemorrhage in HIPs (10/11) was significantly higher than that in non-HIPs (9/25, Fig. 1C). PMR values in plaques with intraplaque hemorrhage were higher than those without intraplaque hemorrhage (Fig. 1D). The sensitivity and specificity of intraplaque hemorrhage in HIPs were 64% and 91%, respectively. Fig. 2 shows representative $T_1$WI and $T_2$WI of a coronary artery with HIP and corresponding histological images. The high-intensity portions in large coronary plaques on $T_1$WI showed low signal intensity on $T_2$WI. Ten of 11 high-intensity portions on $T_1$WI were variably immunopositive for CD68, glycophorin A, and fibrin. One high-intensity portion on $T_1$WI was immunopositive for CD68 and fibrin but not for glycophorin A. We compared immunopositive areas for CD68, CD163, α-SMA, glycophorin A, fibrin, and Berlin-blue-dye-positive areas. Glycophorin A, fibrin, CD163, and Berlin blue dye are related to intraplaque hemorrhage as an erythrocyte protein, blood coagulation end product, a macrophage haptoglobin–hemoglobin complex receptor, and $Fe^{3+}$-binding dye, respectively. Glycophorin-A-immunopositive areas were larger and α-SMA-immunopositive areas were smaller in HIPs than in non-HIPs. CD68- and fibrin-immunopositive areas tended to be larger in HIPs than in non-HIPs, but this was not significant. There was no significant difference in Berlin-blue-dye-positive iron deposition between the groups (Fig. 3). No immunoreaction for nonimmune mouse or rabbit immunoglobulin G was observed.

To examine the biological significance of coronary HIPs on $T_1$WI, the corresponding sections were stained with antibodies for MMP9, a marker of plaque instability, and tissue factor, a marker of the thrombogenic potential of plaques. MMP9 was predominantly localized in the necrotic core and macrophages surrounding the necrotic core. Tissue factor was expressed in macrophages and smooth muscle cells as multiple foci in plaques (Fig. 2). MMP9- and tissue factor-immunopositive areas were larger in HIPs than in non-HIPs (Fig. 3).

We next examined the association between the PMR and immunopositive areas in coronary plaques (Table 1). The PMR was positively correlated with glycophorin-A- ($r=0.35$), fibrin- ($r=0.35$), MMP9- ($r=0.33$), and tissue factor-immunopositive ($r=0.37$) areas.

We performed in vitro blood MRI to examine the contribution of blood contents or blood coagulation to HIPs on $T_1$WI. Supplementary Table 2 shows the cell counts in whole blood, plasma, and plasma-removed centrifuged blood. The numbers of erythrocytes in whole blood, plasma, and centrifuged blood were $4.5\pm1.2\times10^6$/μl, 0/μl, and $7.5\pm3.5\times10^6$/μl, respectively. Fig. 4A and B shows in vitro $T_1$WI and $T_1$ mapping of whole blood, plasma, and centrifuged blood with or without coagulation. Coagulation reduced the $T_1$ value and enhanced signal intensity in blood. Noncoagulated whole blood and centrifuged blood showed high signal intensity on $T_1$WI compared with plasma. Fig. 4C and D shows $T_1$ relaxation times in noncoagulated or coagulated whole blood, plasma, and centrifuged blood. $T_1$ relaxation times in noncoagulated and coagulated whole blood and centrifuged blood were significantly shorter than those in plasma.

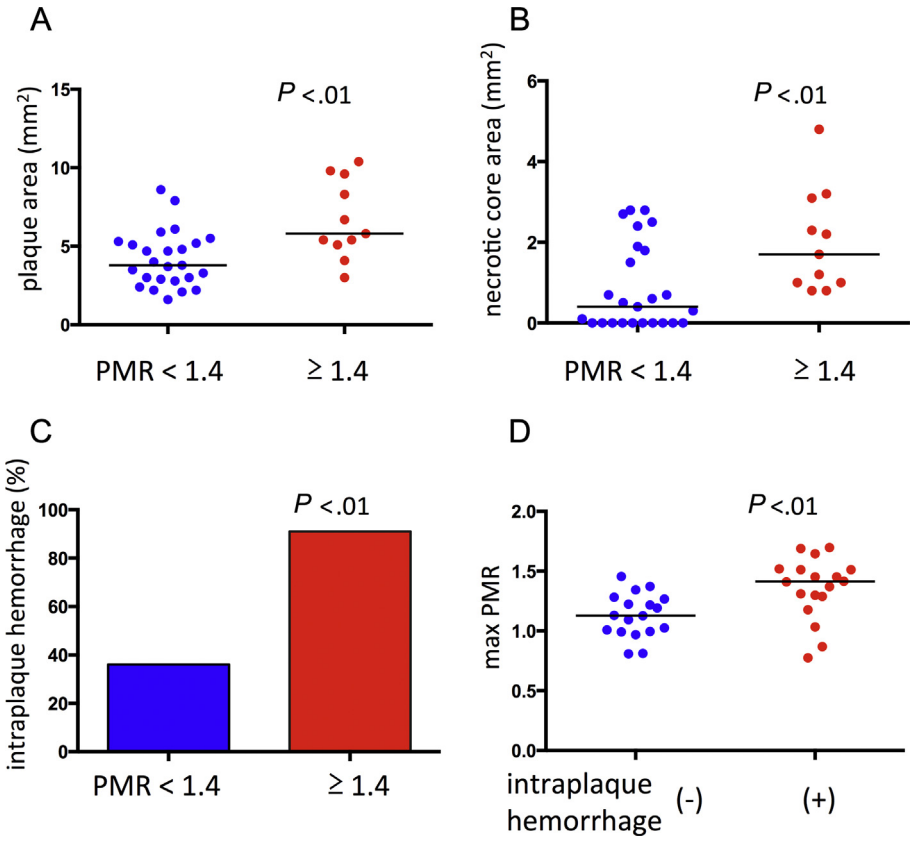


**Fig. 1.** Histological characteristics of HIPs. Histological plaque area (A), necrotic core area (B), and the frequency of intraplaque hemorrhage (C) in non-HIPs (PMR <1.4, $n=25$, blue dots) and in HIPs (PMR ≥1.4, $n=11$, red dots). (D) Values of the PMR in plaques with or without intraplaque hemorrhage. The Mann–Whitney *U* test was used to analyze plaque and necrotic core areas and the maximum PMR value, and Fisher's Exact Test was used for the frequency of intraplaque hemorrhage. HIP = high-signal-intensity plaque, PMR = plaque to myocardial signal intensity ratio.

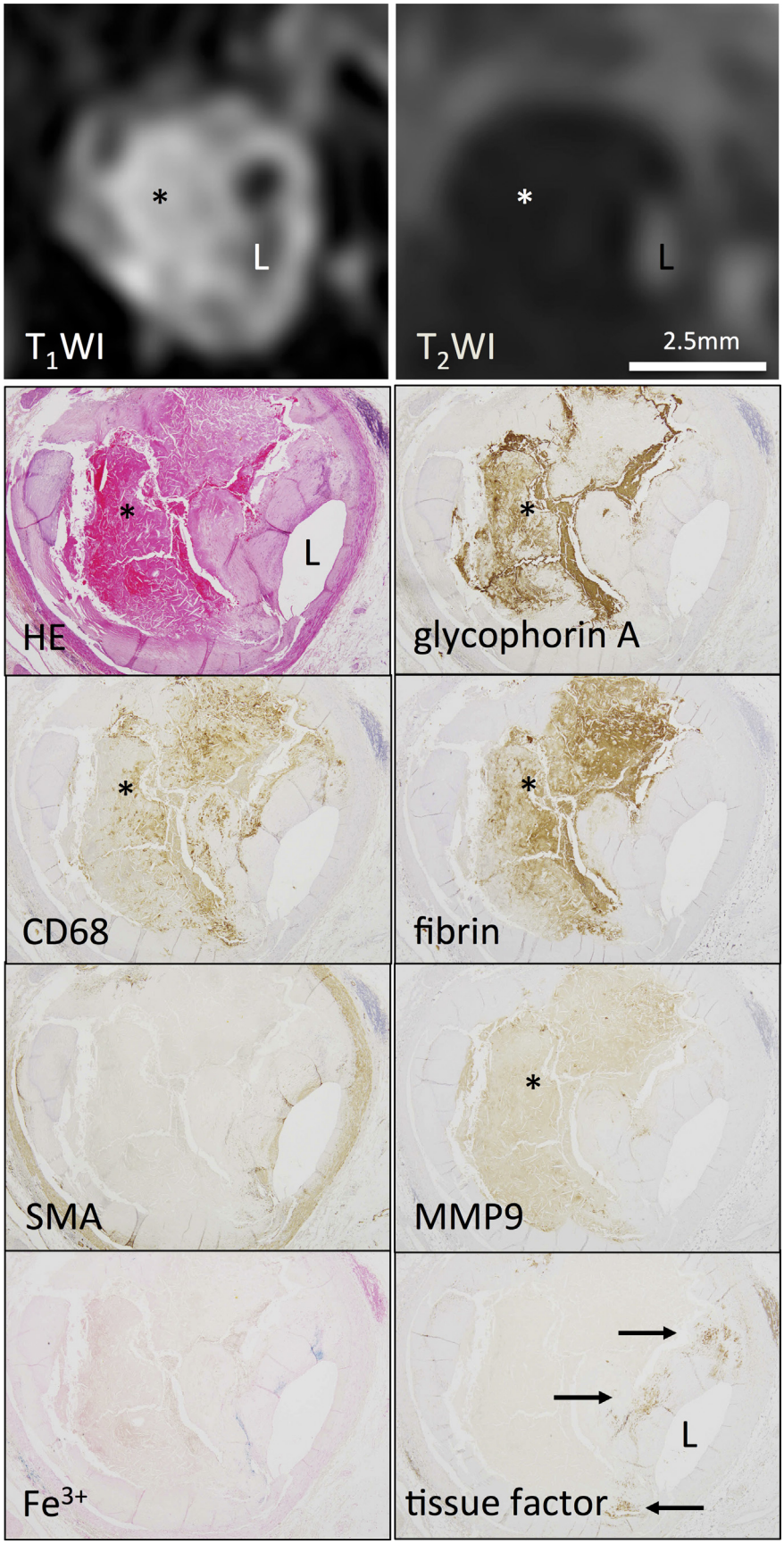


**Fig. 2.** Representative $T_1$WI, $T_2$WI, and histological and immunohistochemical images of an HIP. The $T_1$ high-intensity portions (asterisks) in a plaque show low signal intensity on $T_2$WI and are variably immunopositive for CD68, glycophorin A, fibrin, and MMP9. Tissue factor-immunopositive foci in a plaque can be seen (arrows). The foci are close to the lumen (L). MMP = matrix metalloproteinase, $T_1$WI = $T_1$-weighted imaging, $T_2$WI = $T_2$-weighted imaging.

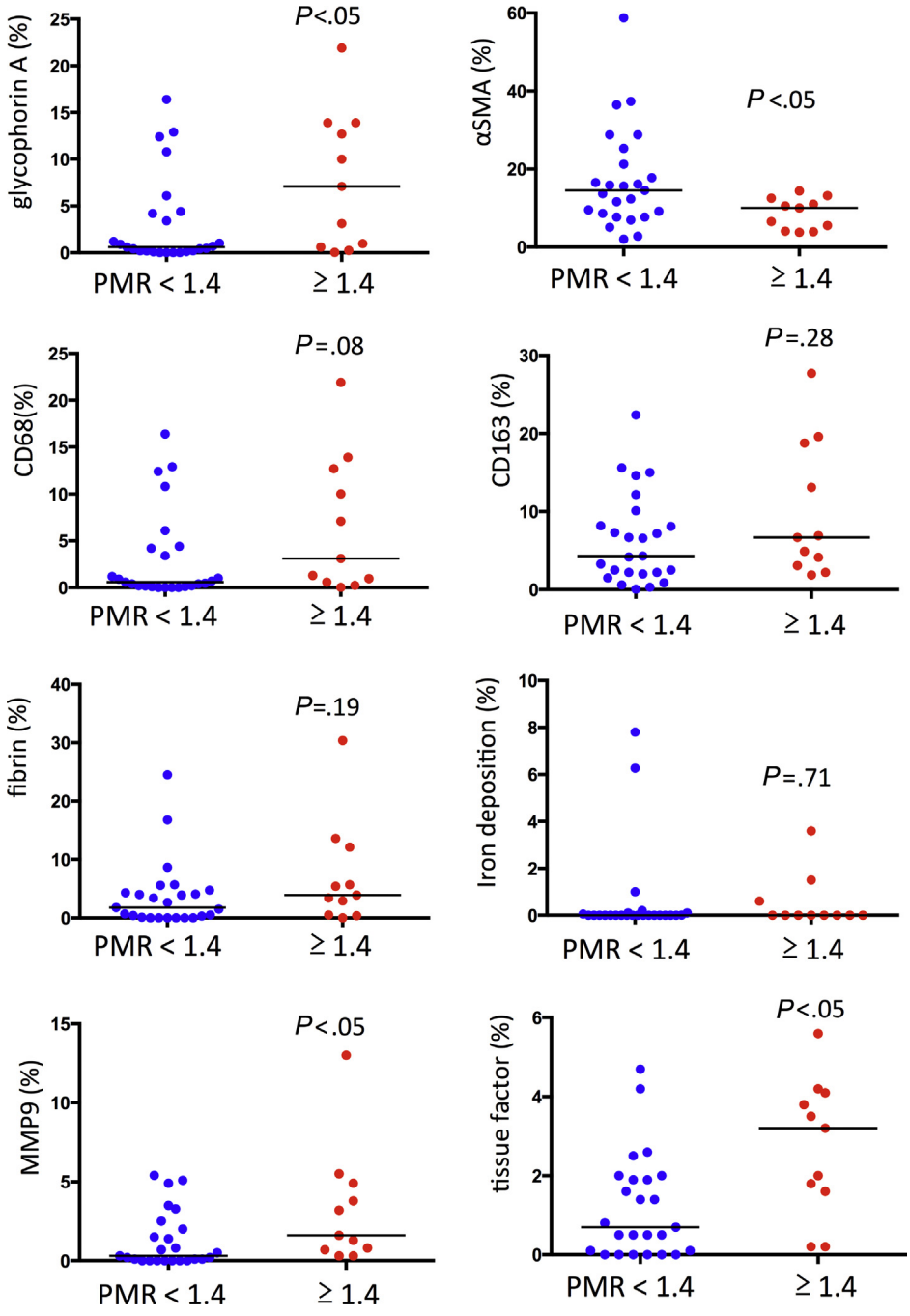


**Fig. 3.** Immunopositive or Berlin-blue-dye-positive areas in non-HIPs (PMR <1.4, $n$=25, blue dots) and in HIPs (PMR ≥1.4, $n$=11, red dots). The Mann–Whitney $U$ test was used for analysis.

**Table 1**
Relationship between PMR and stained area

| | PMR | |
|---|---|---|
| | Correlation coefficient | $P$ value |
| Glycophorin A (%) | 0.35 | <.05 |
| αSMA (%) | −0.18 | .3 |
| CD68 (%) | 0.25 | .14 |
| CD163 (%) | 0.19 | .25 |
| Fibrin (%) | 0.35 | <.05 |
| Iron deposition (%) | −0.04 | .83 |
| MMP9 (%) | 0.33 | <.05 |
| Tissue factor (%) | 0.37 | <.05 |

MMP, matrix metalloproteinase; PMR, plaque to myocardial signal intensity ratio; SMA, smooth muscle actin ($n$=36).

## 4. Discussion

We showed that the majority of HIPs had intraplaque hemorrhage in the large necrotic core and that the PMR was positively correlated with erythrocyte-, fibrin-, MMP9-, and tissue factor-immunopositive areas. In vitro MRI showed that blood coagulation and erythrocyte content shortened the $T_1$ relaxation time.

Several clinical studies investigated the characteristics of HIPs with CT, intravascular ultrasound, OCT, and coronary angioscopy in patients with angina pectoris. Kawasaki et al. [6] examined 25 lesions from 24 patients with angina pectoris and showed a higher frequency of positive remodeling and lower CT density in HIPs (defined as a PMR >1.0). Ehara et al. [10] examined morphological characteristics of HIPs (defined as a PMR >1.0) in 26 lesions from 26 patients with stable or unstable angina.

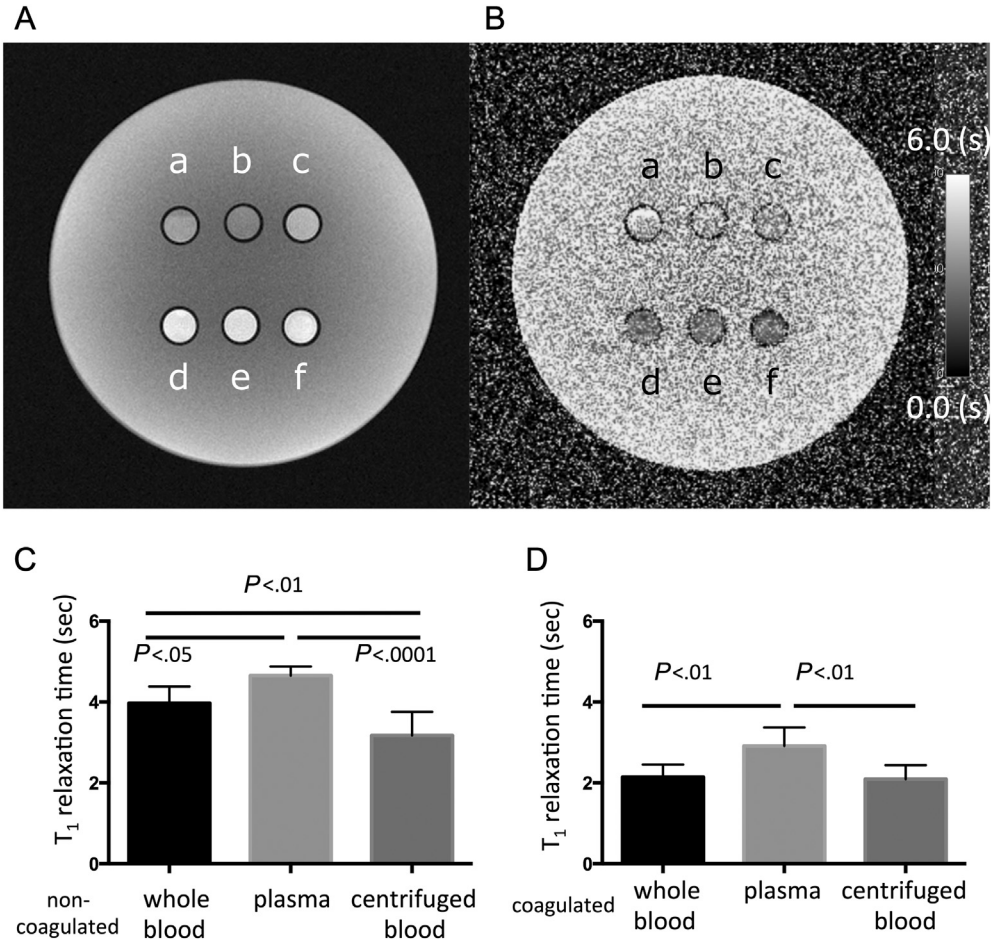


**Fig. 4.** In vitro $T_1$WI, $T_1$ mapping, and $T_1$ relaxation time of noncoagulated or coagulated blood. Sodium-citrate-treated human venous blood was divided into whole blood, plasma, and plasma-removed centrifuged blood. Blood coagulation was initiated by human placental tissue factor and $CaCl_2$ solution. (A, B) Representative in vitro $T_1$WI (A) and $T_1$ mapping (B) of noncoagulated (a–c) or coagulated (d–f) whole blood (a, d), plasma (b, e), and centrifuged blood (c, f). (C, D) $T_1$ relaxation time of noncoagulated (C) and coagulated (D) whole blood, plasma, and centrifuged blood ($n$=7 in each, one-way analysis of variance and a multiple comparison test were used for analysis).

They found that HIPs (defined as a PMR >1.0) were related to OCT-defined coronary thrombus but not thin-cap fibroatheroma, plaque rupture, and calcification. Oshita et al. [11] examined 17 lesions from 17 patients with stable or unstable angina pectoris with coronary angioscopy. These authors showed a higher frequency of thrombus and more plaques of yellow color grade in HIPs (defined as a PMR ≥1.4) than in non-HIPs. The yellow color grade of plaques is an indicator of their instability. High-grade yellow plaques have a prevalence of positive remodeling and a high probability of disruption [12,13]. These clinical studies suggest that coronary HIPs are associated with a vulnerable plaque morphology or luminal thrombus after plaque disruption. In this study, we excluded thrombotic plaques and confirmed the vulnerable plaque morphology of HIPs (PMR ≥1.4). Moody et al. [14] performed a histological validation study in 63 patients who underwent MRI before carotid endarterectomy. Thirty-seven of 40 carotid HIPs were related to complicated (American Heart Association Type VI) plaques, thrombotic plaques, and intraplaque hemorrhage. Although the definition of HIPs is not standardized, our results suggest that large atheromatous plaques with intraplaque hemorrhage are the predominant pathology of coronary HIPs on $T_1$WI. Additionally, our results suggest that a minority of HIPs on $T_1$WI reflect fibrin deposition without intraplaque hemorrhage. A case of pathology of embolus derived from coronary HIP has been reported [15]. Coronary embolic tissue after stent implantation at a HIP consisted of an acute phase thrombus with necrotic core tissue that was rich in foamy macrophages. We observed macrophage infiltrates in HIPs (Fig. 2). However, CD68- and CD163-positive cell contents did not differ between HIPs and non-HIPs. Although macrophages are an important component of plaques, our results suggest that macrophages have a limited effect on $T_1$ signal intensity.

Intraplaque hemorrhage is a finding with advanced atherosclerotic plaques, and it may originate from plaque rupture or fissure and leakage from intraplaque vessels. Intraplaque hemorrhage might contribute to expansion and progression of plaques via free cholesterol accumulation, but its role in plaque instability is controversial. In coronary arteries, late-necrotic core fibroatheromas and thin-cap fibroatheromas show a marked increase in glycophorin A in regions of cholesterol clefts surrounded by iron deposition compared with lesions with pathological intimal thickening or early necrotic core fibroatheromas [8]. Additionally, a previous study demonstrated that rabbit aortic atheroma injected with autologous erythrocytes showed more extensive macrophage infiltration, lipid content, and cholesterol crystal formation compared with control rabbits [8]. Intraplaque hemorrhage, iron deposition, and thrombus formation are greater in coronary plaques from patients with unstable versus stable angina pectoris. Oxidized low-density lipoprotein content and expression of thioredoxin, an antioxidative protein, are positively correlated with iron deposition [16]. Intracellular or extracellular deposition of transition metal iron ($Fe^{2+}$ and $Fe^{3+}$) derived from erythrocytes can be a potent source of hydroxyl radical (•OH) generation via the Fenton reaction [17]. Therefore, intraplaque hemorrhage may contribute to some aspect of coronary thrombosis via a redox reaction. In contrast, Boyle et al. [18] found a novel macrophage phonotype

in human advanced plaques with intraplaque hemorrhage. Hemorrhage-associated macrophages showed increased expression of heme oxygenase 1, CD163, and interleukin (IL)-10 and suppressed oxidative stress. Hemoglobin suppresses foam cell formation via liver X receptor α activation and macrophage reverse cholesterol transport [19]. Heme oxygenase 1 induction by hemin inhibits progression of atherosclerotic lesions with a change into more stable plaque morphology via a reduction in MMP9 and IL-6 levels and an increase in IL-10 levels [20]. In our study, MMP9 and tissue factor expression in plaques was positively correlated with the PMR on $T_1$WI. Based on the present results and a high cardiovascular event risk in patients with HIPs, hemorrhagic plaques may have biologically unstable and procoagulant potential.

In our study, five coronary plaques with high glycophorin A or fibrin values were found in the non-HIP group. Three of the five plaques showed a high value of iron deposition, which may negatively affect signal intensity on $T_1$WI. CD163 can be induced by the hemoglobin–haptoglobin complex [18]. However, CD163 expression was not associated with HIPs and signal intensity. The present results suggest that HIPs reflect a relatively early phase of intraplaque hemorrhage with intact erythrocytes. Furthermore, the PMR in the five plaques ranged from 1.18 to 1.37 (median: 1.30). The PMR cutoff value of 1.4 may have underestimated intraplaque hemorrhage and fibrin deposition.

$T_1$ relaxation time is affected by methemoglobin content and hematocrit [21,22]. Ebisu et al. [21] examined $T_1$ and $T_2$ relaxation times in nonacute subdural hematomas in vitro. They found that inverted $T_1$ values were positively correlated with the hematocrit and methemoglobin concentrations but not oxyhemoglobin and deoxyhemoglobin concentrations. Although we could not determine the hemoglobin status in plaques, our finding of shorter $T_1$ relaxation times in whole blood and centrifuged blood is comparable with previous studies [21,22]. The low signal intensity on $T_2$WI at high signal intensity on $T_1$WI is compatible with the presence of intracellular methemoglobin. The majority of HIPs on $T_1$WI may reflect methemoglobin within erythrocytes. Interestingly, blood clotting itself shortens $T_1$ relaxation times in blood and plasma, although the exact mechanisms remain unclear. Increased tissue factor expression in plaques can promote blood coagulation after hemorrhage or plasma leakage and may enhance the signal intensity of hemorrhagic plaques or plasma-leaked plaques on $T_1$WI.

HIP on $T_1$WI will be continued for a long time in coronary atherosclerotic plaques. A serial noncontrast $T_1$-weighted MRI study showed that the coronary PMR significantly increased from 1.22 to 1.49 in a 12-month follow-up in the control group but not in the statin-treated group [23]. In this study, the necrotic core area was larger and the α-SMA-immunopositive area was smaller in HIPs than in non-HIPs. Therefore, a delayed organization process in HIPs could affect the finding. We recently examined 137 lesions in 105 patients with stable angina pectoris or silent myocardial ischemia with OCT and a 3-T MRI system [7]. We showed that healed plaque rupture was significantly higher in the HIP group (defined as a PMR ≥1.4) than in the non-HIP group. The result suggests that repeated intraplaque hemorrhage induced by clinically silent plaque rupture may affect the lasting of HIPs.

There are several limitations in this study. Our in vitro experiments cannot represent the in vivo status of plaques and the myocardium. A prospective study with directional coronary atherectomy may provide important information on the pathology of HIPs. Formalin fixation may have affected signal intensity in the coronary arteries and hearts because formalin fixation leads to a reduction in $T_1$ relaxation time in the human brain [24]. To reduce this fixation effect, we calculated the PMR ratio.

In conclusion, the majority of coronary HIPs on $T_1$WI may reflect intraplaque hemorrhage and have biologically unstable and procoagulant potential.

Supplementary data to this article can be found online at https://doi.org/10.1016/j.carpath.2019.01.002.

## Acknowledgments

We are grateful to Ms. Ritsuko Sotomura and Ms. Kyoko Ohashi for their excellent technical assistance and Dr. Taketoshi Asanuma for technical advice.

## Disclosures

Satoshi Yasuda received lecture fees from Takeda Pharmaceutical Company Limited, Daiichi Sankyo Company Limited, and Bristol-Myers Squibb; received research funds from Takeda Pharmaceutical Company Limited and Abbott; and received scholarship funds from Daiichi Sankyo Company Limited. The other authors have no conflicts of interest.

## Funding

This work was supported in part by Grants-in-Aid for Scientific Research in Japan (16K08670, 16H05163, 16K09019) from the Ministry of Education, Culture, Sports, Science and Technology of Japan; the Intramural Research Fund (25-4-3) for Cardiovascular Diseases from the National Cerebral and Cardiovascular Center; and the Clinical Research Fund from Miyazaki University Hospital.

## References

[1] Roth GA, Johnson C, Abajobir A, Abd-Allah F, Abera SF, Abyu G, et al. Global, regional, and national burden of cardiovascular diseases for 10 causes, 1990 to 2015. J Am Coll Cardiol 2017;70:1–25.
[2] Motoyama S, Sarai M, Harigaya H, Anno H, Inoue K, Hara T, et al. Computed tomographic angiography characteristics of atherosclerotic plaques subsequently resulting in acute coronary syndrome. J Am Coll Cardiol 2009;54:49–57.
[3] Rominger A, Saam T, Wolpers S, Cyran CC, Schmidt M, Foerster S, et al. 18F-FDG PET/CT identifies patients at risk for future vascular events in an otherwise asymptomatic cohort with neoplastic disease. J Nucl Med 2009;50:1611–20.
[4] Figueroa AL, Abdelbaky A, Truong QA, Corsini E, MacNabb MH, Lavender ZR, et al. Measurement of arterial activity on routine FDG PET/CT images improves prediction of risk of future CV events. J Am Coll Cardiol Img 2013;6:1250–9.
[5] Noguchi T, Kawasaki T, Tanaka A, Yasuda S, Goto Y, Ishihara M, et al. High-intensity signals in coronary plaques on noncontrast $T_1$-weighted magnetic resonance imaging as a novel determinant of coronary events. J Am Coll Cardiol 2014;63:989–99.
[6] Kawasaki T, Koga S, Koga N, Noguchi T, Tanaka H, Koga H, et al. Characterization of hyperintense plaque with noncontrast $T_1$-weighted cardiac magnetic resonance coronary plaque imaging: comparison with multislice computed tomography and intravascular ultrasound. J Am Coll Cardiol Img 2009;2:720–8.
[7] Kanaya T, Noguchi T, Otsuka F, Asaumi Y, Kataoka Y, Morita Y, et al. Optical coherence tomography-verified morphological correlates of high-intensity coronary plaques on non-contrast T1-weighted magnetic resonance imaging in patients with stable coronary artery disease. Eur Heart J Cardiovasc Imaging 2018. https://doi.org/10.1093/ehjci/jey035.
[8] Kolodgie FD, Gold HK, Burke AP, Fowler DR, Kruth HS, Weber DK, et al. Intraplaque hemorrhage and progression of coronary atheroma. N Engl J Med 2003;349:2316–25.
[9] Rosset A, Spadola L, Ratib O. OsiriX: an open-source software for navigating in multidimensional DICOM images. J Digit Imaging 2004;17:205–16.
[10] Ehara S, Hasegawa T, Nakata S, Matsumoto K, Nishimura S, Iguchi T, et al. Hyperintense plaque identified by magnetic resonance imaging relates to intracoronary thrombus as detected by optical coherence tomography in patients with angina pectoris. Eur Heart J Cardiovasc Imaging 2012;13:394–9.
[11] Oshita A, Kawakami H, Miyoshi T, Seike F, Matsuoka H. Characterization of high-intensity plaques on noncontrast $T_1$-weighted magnetic resonance imaging by coronary angioscopy. J Cardiol 2017;70:520–3.
[12] Uchida Y, Nakamura F, Tomaru T, Morita T, Oshima T, Sasaki T, et al. Prediction of acute coronary syndromes by percutaneous coronary angioscopy in patients with stable angina. Am Heart J 1995;130:195–203.
[13] Takano M, Mizuno K, Okamatsu K, Yokoyama S, Ohba T, Sakai S. Mechanical and structural characteristics of vulnerable plaques: analysis by coronary angioscopy and intravascular ultrasound. J Am Coll Cardiol 2001;38:99–104.
[14] Moody AR, Murphy RE, Morgan PS, Martel AL, Delay GS, Allder S, et al. Characterization of complicated carotid plaque with magnetic resonance direct thrombus imaging in patients with cerebral ischemia. Circulation 2003;107:3047–52.
[15] Asaumi Y, Noguchi T, Morita Y, Matsuyama TA, Otsuka F, Fujiwara R, et al. Noncontrast $T_1$-weighted magnetic resonance imaging at 3.0 tesla in a patient undergoing elective percutaneous coronary intervention — clinical and pathological significance of high-intensity plaque. Circ J 2015;79:218–20.
[16] Nishihira K, Yamashita A, Imamura T, Hatakeyama K, Sato Y, Nakamura H, et al. Thioredoxin in coronary culprit lesions: possible relationship to oxidative stress and intraplaque hemorrhage. Atherosclerosis 2008;201:360–7.

[17] Madamanchi NR, Vendrov A, Runge MS. Oxidative stress and vascular disease. Arterioscler Thromb Vasc Biol 2005;25:29–38.
[18] Boyle JJ, Harrington HA, Piper E, Elderfield K, Stark J, Landis RC, et al. Coronary intraplaque hemorrhage evokes a novel atheroprotective macrophage phenotype. Am J Pathol 2009;174:1097–108.
[19] F inn AV, Nakano M, Polavarapu R, Karmali V, Saeed O, Zhao X, et al. Hemoglobin directs macrophage differentiation and prevents foam cell formation in human atherosclerotic plaques. J Am Coll Cardiol 2012;59:166–77.
[20] Li T, Tian H, Zhao Y, An F, Zhang L, Zhang J, et al. Heme oxygenase-1 inhibits progression and destabilization of vulnerable plaques in a rabbit model of atherosclerosis. Eur J Pharmacol 2011;672:143–52.
[21] Ebisu T, Naruse S, Horikawa Y, Tanaka C, Higuchi T. Nonacute subdural hematoma: fundamental interpretation of MR images based on biochemical and in vitro MR analysis. Radiology 1989;171:449–53.
[22] Blackmore CC, Francis CW, Bryant RG, Brenner B, Marder VJ. Magnetic resonance imaging of blood and clots in vitro. Invest Radiol 1990;25:1316–24.
[23] Noguchi T, Tanaka A, Kawasaki T, Goto Y, Morita Y, Asaumi Y, et al. Effect of intensive statin therapy on coronary high-intensity plaques detected by noncontrast T1-weighted imaging: the AQUAMARINE pilot study. J Am Coll Cardiol 2015;66:245–56.
[24] Schmierer K, Thavarajah JR, An SF, Brandner S, Miller DH, Tozer DJ. Effects of formalin fixation on magnetic resonance indices in multiple sclerosis cortical gray matter. J Magn Reson Imaging 2010;32:1054–60.